EFFECT OF DILUTION ON THE PROPERTIES OF THE DISSIMILAR JOINT BETWEEN AUSTENITIC AND FERRITIC STAINLESS STEELS

G.A. Nassef
Production Engineering Department, Faculty of engineering,
Alexandria University, Alexandria, Egypt.

ABSTRACT

Dissimilar fusion metal welds have been created between type 304 austenitic steel and type 430 ferritic steel using gas tungsten arc. Three types of stainless steel welding rods being ER308L, ER309L and ER310 have been used. The dilution effect on the microstructure and mechanical properties of the weld deposits has been characterized. It is found that the critical section of the as-weld ***deposits*** is the interface between the weld metal and ferritic stainless steel base metal. Exceptionally low as-weld toughness has been reported at the ferritic steel-weld interface using type ER308L electrode. This has been attributed to the formation of martensite in the microstructure as a result of dilution of weld metal with ferritic steel base metal. The degradation of Charpy toughness and tensile strength due to aging at 600 ^{0}C for different exposures has been investigated. A drastic decrease of Charpy toughness with aging time has been reported at the ferritic steel-weld interface for the weld deposit of type ER309L. This has been attributed to the higher tendency of this ferrite-rich weld metal structure to undertake ferrite-sigma phase transformation. The heat affected zone of ferritic steel showed the lowest tensile strength of the as-weld *joints*. Aging for more than 20 hr resulted in tensile failure at the ferritic steel-weld interface for joints corresponding to types ER308L and ER309L electrodes. For the investigated aging conditions, the joints of Type ER310 electrode failed in tension eventually inside the heat affected zone of ferritic steel.

Keywords: Materials Technology, Welding, Dissimilar joints, Stainless Steels.

1. INTRODUCTION

Dissimilar metal welds (DMW's) between austenitic and ferritic steel tubing and piping are commonly employed at high temperature applications in energy conversion systems. In power generating plants, austenitic stainless steels are used in high temperature superheaters and reheaters because of their good creep and corrosion resistance. For economic reasons, ferritic steels are employed where temperature is lower so that a dissimilar weld joint is needed. Dissimilar welds are also used in main steam lines of fossil boilers, in gas-cooled reactors, in fast-breeder reactors, and in petrochemical plants.

Differences in coefficient of thermal expansion (CTE) between the two types of stainless steel induce thermal stresses in the weld metal and local metallurgical changes near the interface between the ferritic steel and the weld metal. These phenomena together with the differences in creep behavior of the materials joined, render the dissimilar joints more prone to failure than welds between similar stainless steels. Various approaches have been conducted to circumvent the problem of different coefficients of thermal expansion. One approach [1] is to use a tri-metallic transition joint where the transition piece having a coefficient of thermal expansion layimg between those of ferritic steel and austenitic steel. The nickel base weld metal has a CTE value between those of the ferritic and austenitic base metals. The use of nickel base weld metal in welding dissimilar stainless steel did not exclude the premature service failure [1-3]. Nucleation and propagation of fatigue cracks along a planer array of globular carbides are considered responsible for this type of failure.

Dilution is another important factor that plays a major role in influencing the in-service high temperature behavior of DMWs. An important aspect of the dilution is the effect it has on the weld-metal microstructure. When two metals are fusion welded together, the final

composition consists of an admixture of the materials of the parent metal and the welding wire. In other words some of the parent plate is melted and dilutes the molten filler metal. Several techniques have been employed to determine the weld metal composition in DMWs. The most accurate of these is the chemical analysis of a sample of weld metal taken at different locations. But this technique is an expensive and time consuming one. Approximation of base metal dilution by weld cross section and composition calculation is another technique based on area measurements, as shown schematically in Figure (1). This technique has been developed later [2,4] to be applied to different welding processes, by assuming different dilution percentage for each particular welding process, as listed in Table (1)

The weight percentage of any element in the weld metal after dilution is determined by the following formula:

$$X_x = X_A \, X \, d + X_B \, x \, d + X_F \, (1\text{-}d) \qquad (1)$$

Where:

X_X is the average percentage of element X in the weld metal

X_A is the percentage of element X in the base metal A.

X_B is the percentage of element X in the base metal B.

X_F is the percentage of the element X in the filler metal

d is the dilution fraction

The influence of high temperature exposure on the interfacial microstructure and mechanical properties of various many dissimilar metal steel welds has been the subject of previous investigation [1-3,5-9]. Thermal creep [10] and thermal fatigue behavior of dissimilar joints [11] have also been characterized through laboratory tests. The evolution of microstructural constituents with service loading at elevated temperature [1] and in laboratory tests [3] has been found to play the predominant role in premature failure. Avery [2] indicated that failures occurring after long service at elevated temperatures have not been related to ordinary welding defects such as slag, lack of fusion or porosity but are related to metallurgical changes due to service conditions.

In this investigation the dilution in dissimilar weld joints between 304 austenitic stainless steel and 430 ferritic stainless steel is to be characterized. The dilution principle is to be employed to predict the interfacial microstructural constituents. The microstructural changes of the diluted weld metal as well as the associated evolution of Charpy toughness and tensile strength with aging at elevated temperature are to be investigated.

2. EXPERIMENTAL PROCEDURE

2.1 *Material*

The dissimilar base metals used in the present investigation are type 304 austenitic stainless steel and type 430 ferritic stainless steel both in the form of sheets of 10 mm thickness . The chemical compositions of the used steels as prescribed by the manufacturer are given in Tables (2&3).

Three types of welding electrodes were used being ER308L, ER309L, and ER310L having the compositions shown in Table (4). These electrodes are especially selected for their different Cr/Ni equivalent ratios, to obtain different interfacial constituents by dilution with the base metals.

2.2 *Welding and specimen preparation*

The as-received plates of the two base metals have been machine cut to produce identical pieces of 200x100x10 mm dimensions. The gas tungsten arc has been used to deposit bead-on-plate weld pads on each of the two base metals as shown in Figure (2). The pads were built up to a height of about 12 mm, by multi-run deposition. The arc properties, electrode diameter, and welding speed (Table 5),were maintained the same for all pads. Single-Vee edge preparation was created by machining the deposited edges as shown in Figure (3). The two parts of the base metals were then joined together by multi-run GTA, using the welding conditions given in Table (5). Standard test specimens for Charpy impact test were taken perpendicular to the weld as shown in Figure (4). The position of Vee-notch in Charpy test specimens was varied to include three locations with respect to the weld- base metal interface as shown in Figure (5). Standard tensile test specimens were taken transverse to the welding line.

Table 1 Dilution percentage assumed for some fusion welding processes

WELDING PROCESS	DILUTION %
Metal Arc	25 to 40
Submerged Arc	25 to 40
MIG (spray transfer)	25 to 50
MIG (dip transfer)	15 to 30
TIG	25 to 50

Table 2 Chemical composition of type 304 austenitic stainless steel as given by the manufacturer

ELEMENT	C	Si	Mn	P	S	Ni	Cr
Wt.%	0.06	0.59	1.02	0.032	0.013	8.56	18.40

Table 3 Chemical composition of type 430 ferritic stainless steel as given by the manufacturer

ELEMENT	C	Si	Mn	P	S	Ni	Cr
Wt.%	0.06	0.70	0.48	0.026	0.004	-	16.31

Table 4 Chemical composition of the different electrodes as given by the manufacturer

Electrode type (AWS)	C	Si	Mn	Ni	Cr
ER308L	0.02	0.3	1.7	9.7	20.5
ER309L	0.02	0.4	1.5	13	24
ER310	0.1	0.5	1.5	21	26

Table 5 Welding conditions

WELDING PROCESS	SHIELDING GAS	WELDING VOLTAGE	POLARITY	WELDING CURRENT	WELDING SPEED (AVERAGE)	ROD DIM.
GTAW	ARGON	25V	DCEN	90 Amp.	5 cm / min.	3.2 mm

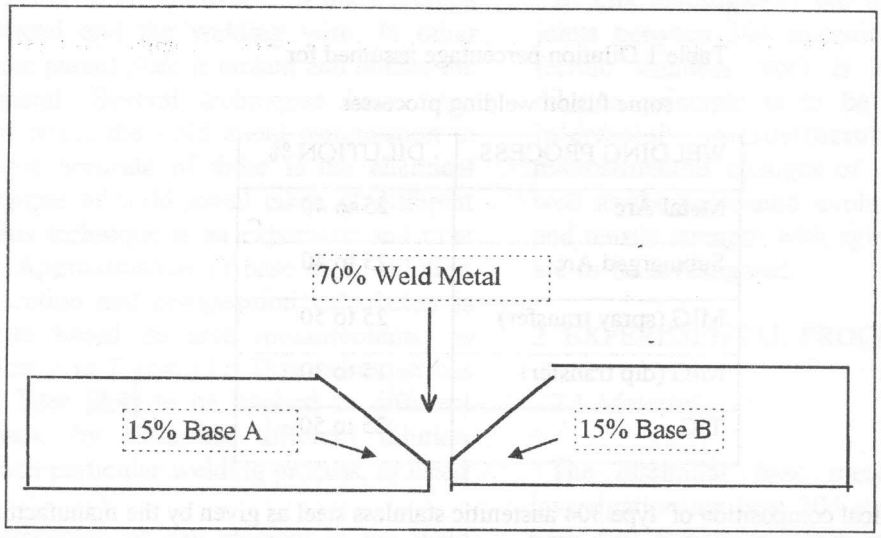

Fig. 1 Dilution of the weld metal by base metals

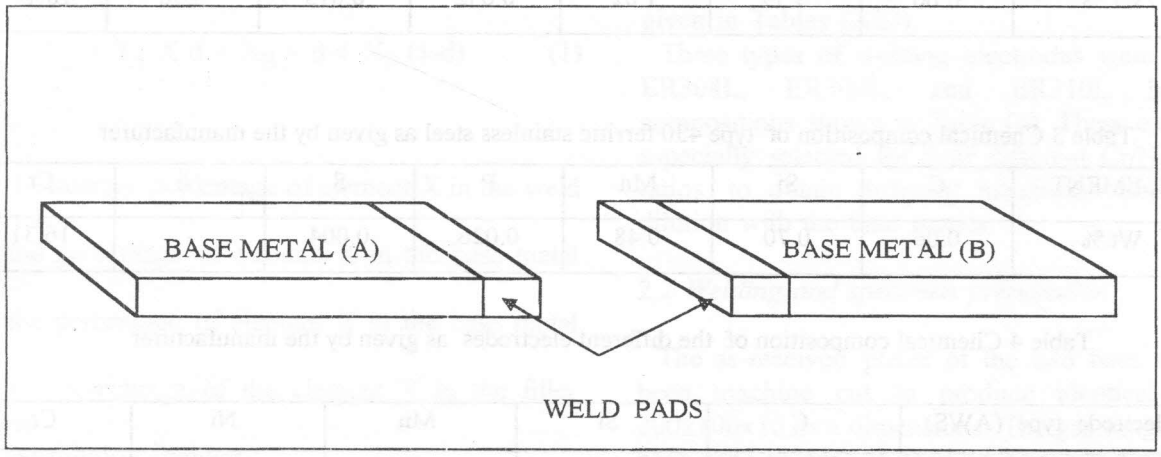

Fig. 2 Deposited weld metal

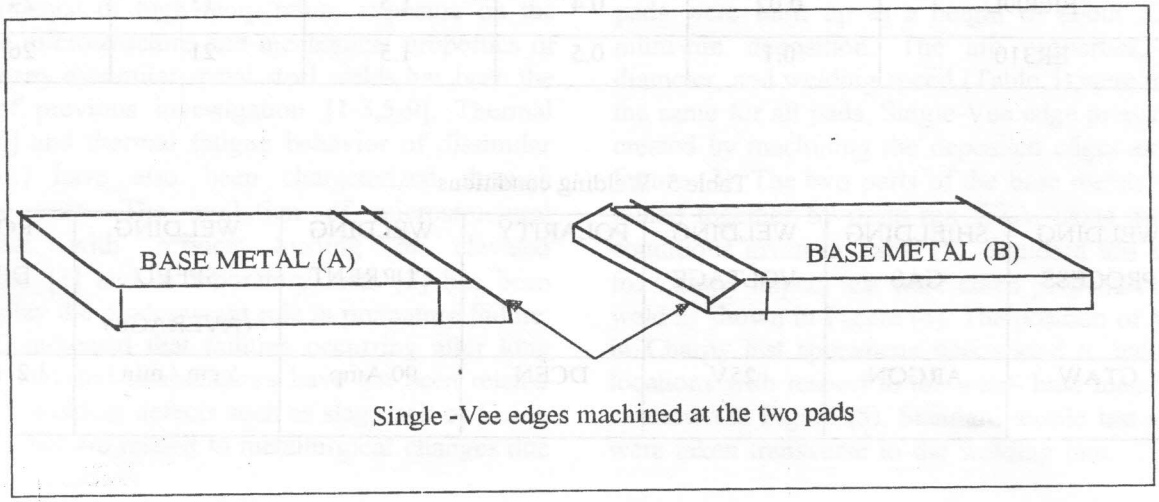

Fig. 3 Single-Vee edge preparation

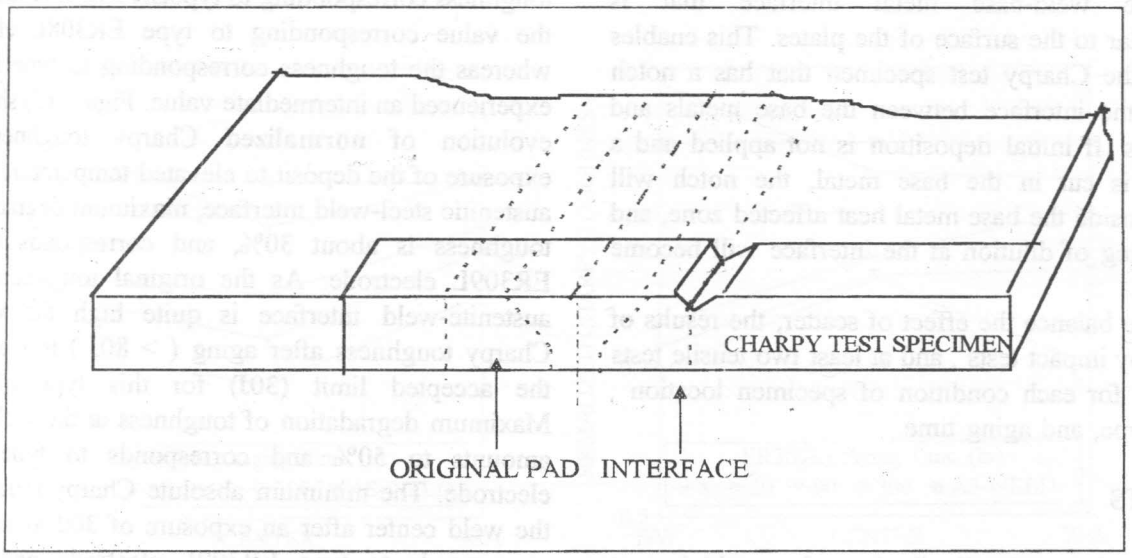

Fig. 4 Charpy impact test specimen taken at the interface between weld metal and base metal

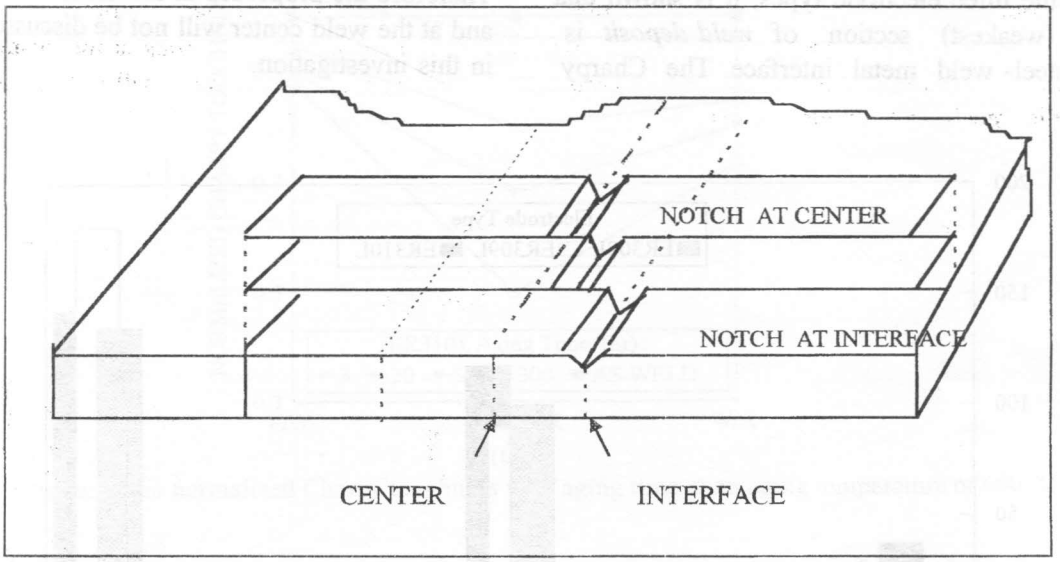

Fig. 5 Locations of Charpy impact test specimens w.r.t the interface

2.3 *Aging*

Both Charpy and tensile test specimens were exposed to elevated temperature of 600 °c for various exposure times of 3, 8, 20, 90, and 300 hr, inside an electrical resistance muffle furnace. This exposure was followed by air cooling to room temperature. Some specimens for microscopic observations were also subjected to the same treatment.

2.4 *Mechanical testing*

The tensile test specimens, both in the as- weld and in the aged conditions, were tested at constant cross head speed of 5 mm / min until failure. Charpy Vee-notched test specimens taken at different locations transversely to the weld were tested in both the as-weld and aged-weld conditions. The initial deposition of weld pads is especially used in the present investigation

to provide weld-base metal interface that is perpendicular to the surface of the plates. This enables testing of the Charpy test specimen that has a notch located at the interface between the base metals and weld metals. If initial deposition is not applied and a single-vee is cut in the base metal, the notch will propagate inside the base metal heat affected zone, and impact testing of dilution at the interface will become impossible.

In order to balance the effect of scatter, the results of three Charpy impact tests , and at least two tensile tests were taken for each condition of specimen location , electrode type, and aging time.

3. RESULTS

Figure (6) shows the distribution of as-weld impact Charpy toughness transverse to the dissimilar ***weld deposit***. For the three electrode types, it is shown that the critical (weakest) section of ***weld deposit*** is the ferritic steel- weld metal interface. The Charpy toughness corresponding to typeER 310 is at least twice the value corresponding to type ER308L electrode, whereas the toughness corresponding to type ER309L experienced an intermediate value. Figure (7) shows the evolution of **normalized** Charpy toughness with exposure of the deposit to elevated temperature. At the austenitic steel-weld interface, maximum degradation of toughness is about 30%, and corresponds to Type ER309L electrode. As the original toughness at the austenite-weld interface is quite high the value of Charpy toughness after aging (> 80J) is well above the accepted limit (30J) for this type of joints. Maximum degradation of toughness at the weld center amounts to 50% and corresponds to type ER310 electrode. The minimum absolute Charpy toughness at the weld center after an exposure of 300 hr at 600 ^{0}C corresponds to type ER309L electrode and is also above the acceptable limit for class of material. Therefore the properties at the austenitic steel interface and at the weld center will not be discussed any further in this investigation.

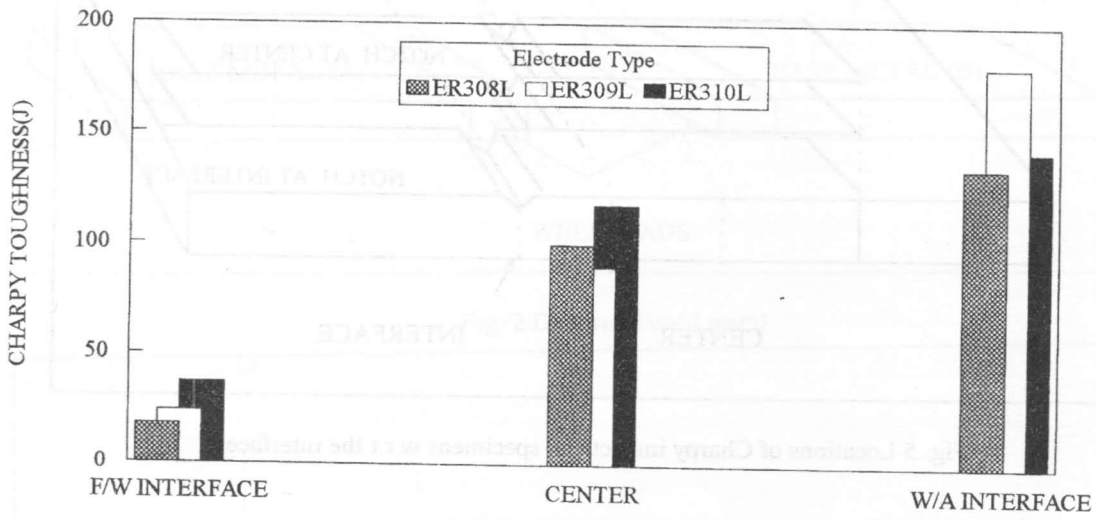

Fig. 6 Distribution of Impact Charpy toughness in the transverse direction normal to the weld joint

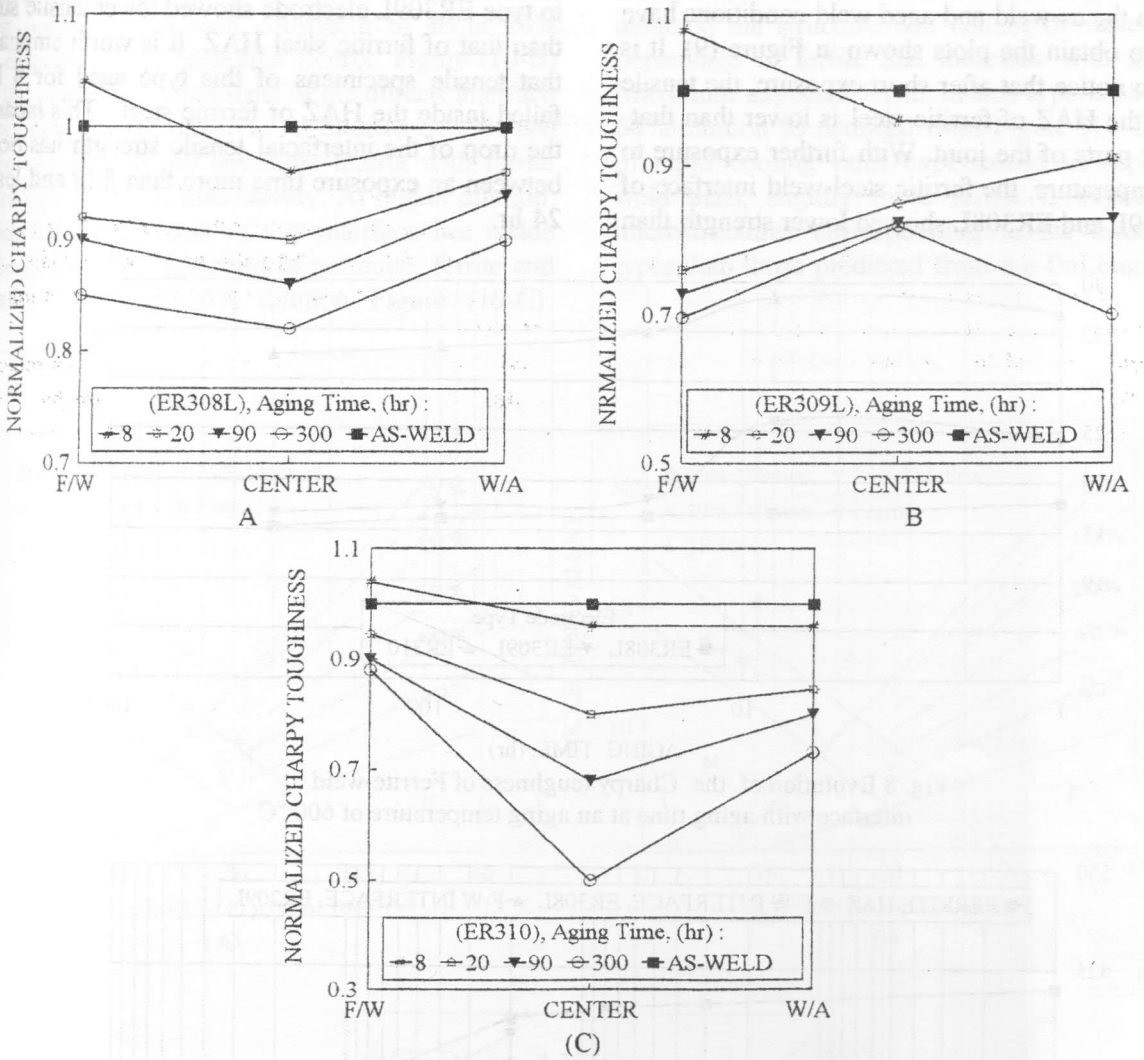

Fig. 7 Evolution of the normalized Charpy toughness with aging time at an aging temperature of 600 °C

Upon exposure to elevated temperature, the toughness at the ferritic steel-weld interface experiences degradation of varying rates depending on the electrode type . Maximum degradation rate occurs at the interface corresponding to type 309L electrode, where the toughness decreases to about 0.68 of the value in the as-weld condition, after an exposure of 300 hr. The most important feature concluded from Figure (7) is that the degradation rate of the interfacial toughness for type 310 electrode decreases with aging time. The evolution of the **absolute** Charpy toughness at the ferritic steel-weld interface for each of the three electrode types is shown in Figure (8). The trend of the results clearly indicates that further exposure beyond 300 hr has a negligible effect on the toughness of the weld interface corresponding to type ER310 electrode.

The tensile test results of the as-weld ***joints*** showed that failure occurs inside the heat affected zone of ferrite. The aged weld specimens corresponding to type ER310 electrode also failed in tension inside the ferrite HAZ for all the investigated range of aging. The location of tensile failure of aged specimens of the two other types of electrode has been found to depend on the aging time. For aging times of 3 and 8 hr., failure for both electrode types was located inside the ferrite heat affected zone. For higher exposure times, tensile

failure occurred in both of the two types by separation at the ferritic steel-weld interface. The results of tensile tests of both the as-weld and aged weld conditions have been used to obtain the plots shown in Figure (9). It is important to notice that after short exposure, the tensile strength of the HAZ of ferritic steel is lower than that of the other parts of the joint. With further exposure to elevated temperature, the ferritic steel-weld interface of types ER309L and ER308L showed lower strength than that of the HAZ. At an exposure time of 24 hr more, the tensile strength of the interface correspond to type ER309L electrode showed lower tensile stren than that of ferritic steel HAZ. It is worth emphasiz that tensile specimens of this type aged for 8 hr failed inside the HAZ of ferritic steel. This means the drop of the interfacial tensile strength has occu between an exposure time more than 8 hr and less t 24 hr.

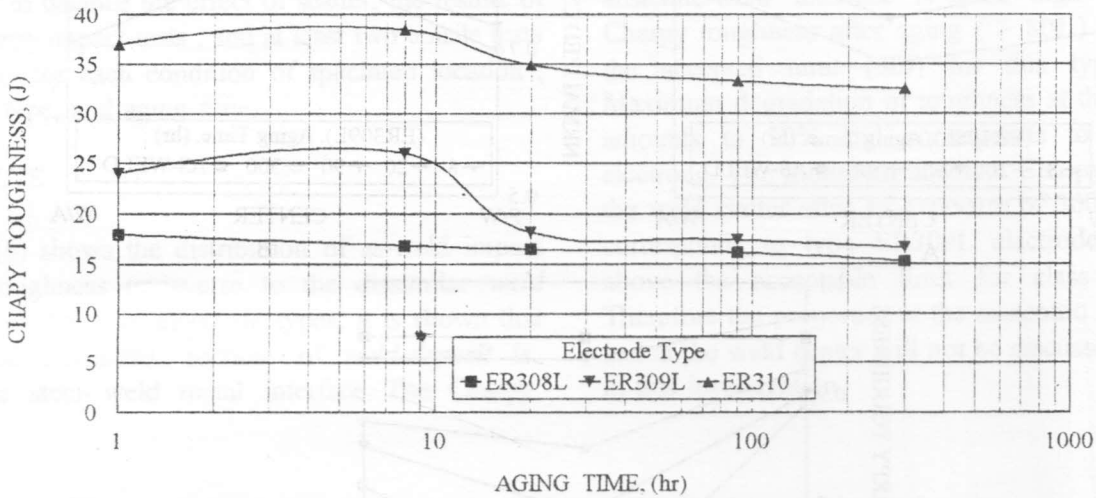

Fig. 8 Evolution of the Charpy toughness of Ferrite-weld interface with aging time at an aging temperature of 600 °C

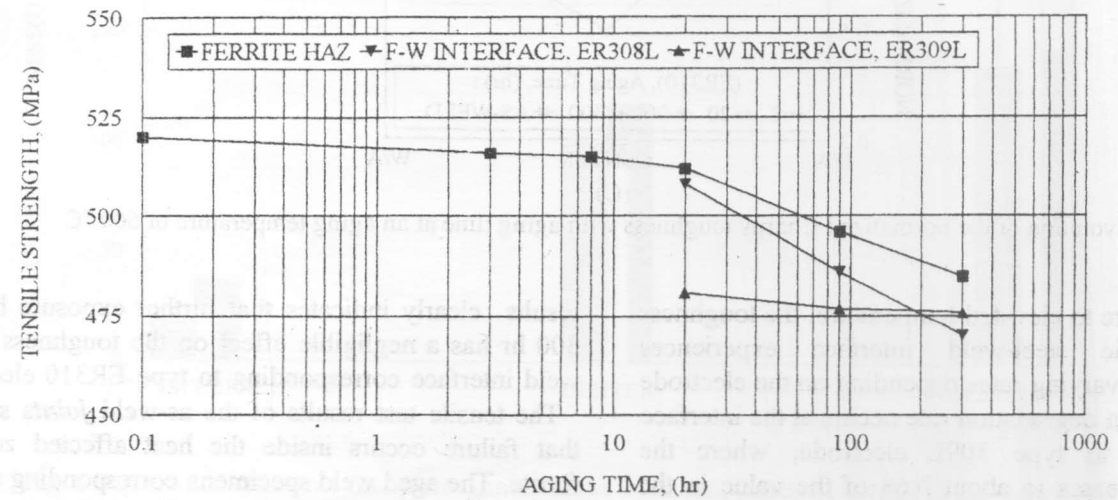

Fig. 9 Evolution of tensile strength of different joint locations with aging time

Equation 1 has been used to predict the chemical composition at the ferritic steel-weld interface assuming different dilution percentage. The results have been used to determine the nickel equivalent and chromium equivalent for each condition of electrode types. The results are plotted on the modified DeLong diagram shown in Figure (10). The dilution effect on interface corresponding to type ER308L is shown Figure (10-A). Except for the lowest dilution, predicted constituents are ferrite, austenite

failure occurred in both of the two types by separation at the ferritic steel-weld interface. The results of tensile tests of both the as-weld and aged weld conditions have been used to obtain the plots shown in Figure (9). It is important to notice that after short exposure, the tensile strength of the HAZ of ferritic steel is lower than that of the other parts of the joint. With further exposure to elevated temperature, the ferritic steel-weld interface of types ER309L and ER308L showed lower strength than that of the HAZ. At an exposure time of 24 hr and more, the tensile strength of the interface corresponding to type ER309L electrode showed lower tensile strength than that of ferritic steel HAZ. It is worth emphasizing that tensile specimens of this type aged for 8 hr has failed inside the HAZ of ferritic steel. This means that the drop of the interfacial tensile strength has occurred between an exposure time more than 8 hr and less than 24 hr.

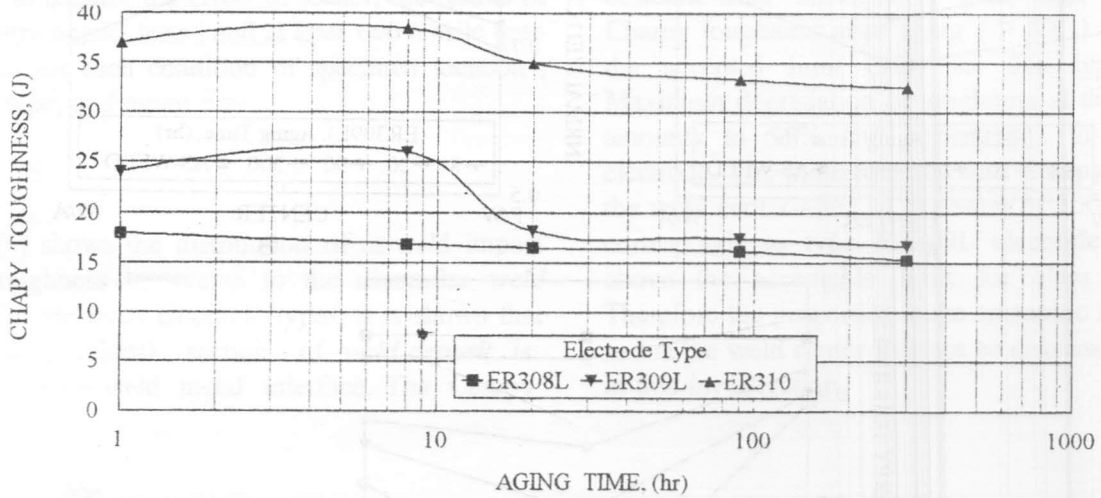

Fig. 8 Evolution of the Charpy toughness of Ferrite-weld interface with aging time at an aging temperature of 600 °C

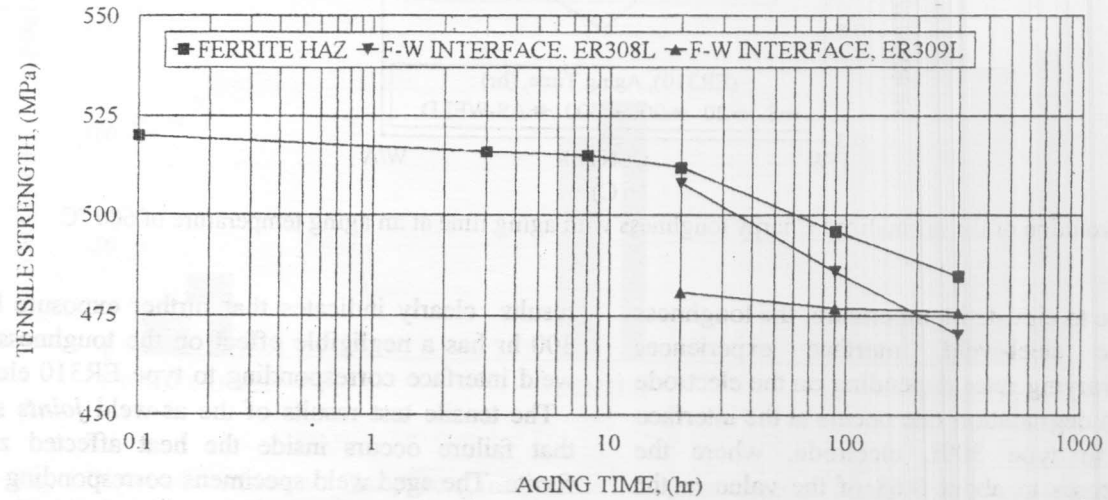

Fig. 9 Evolution of tensile strength of different joint locations with aging time

Equation 1 has been used to predict the chemical composition at the ferritic steel-weld interface assuming different dilution percentage. The results have been used to determine the nickel equivalent and chromium equivalent for each condition of electrode types. The results are plotted on the modified DeLong diagram as shown in Figure (10). The dilution effect on the interface corresponding to type ER308L is shown in Figure (10-A). Except for the lowest dilution, the predicted constituents are ferrite, austenite and

martensite, with percentages of martensite and ferrite increasing with the extent of dilution. The lowest dilution predicts a structure consisting of about 20% ferrite dispersed in an austenitic matrix. Figure (10-B) shows the predicted constituents of the diluted interface corresponding to type ER309L. At dilution of 25% and 40% the constituents are austenitic matrix with ferrite of about 20% and 30% respectively. At higher dilution, the predicted composition of this interface lies inside the three phase zone consisting of austenite, ferrite and martensite. Assuming 25% dilution Figure (10-C) shows for type ER310 electrode that the constituents of the interface is 100% austenite. If higher dilution is assumed the structure will consist of austenite with a percentage of ferrite that increases with the dilution. Maximum expected ferrite in this type is about 15% at 60% dilution as deduced from Figure (10-C). Because of rapid cooling rates experienced in depositing the weld pads, slightly more ferrite is expected in the microstructures corresponding to the three electrode types than those predicted from the DeLong diagrams.

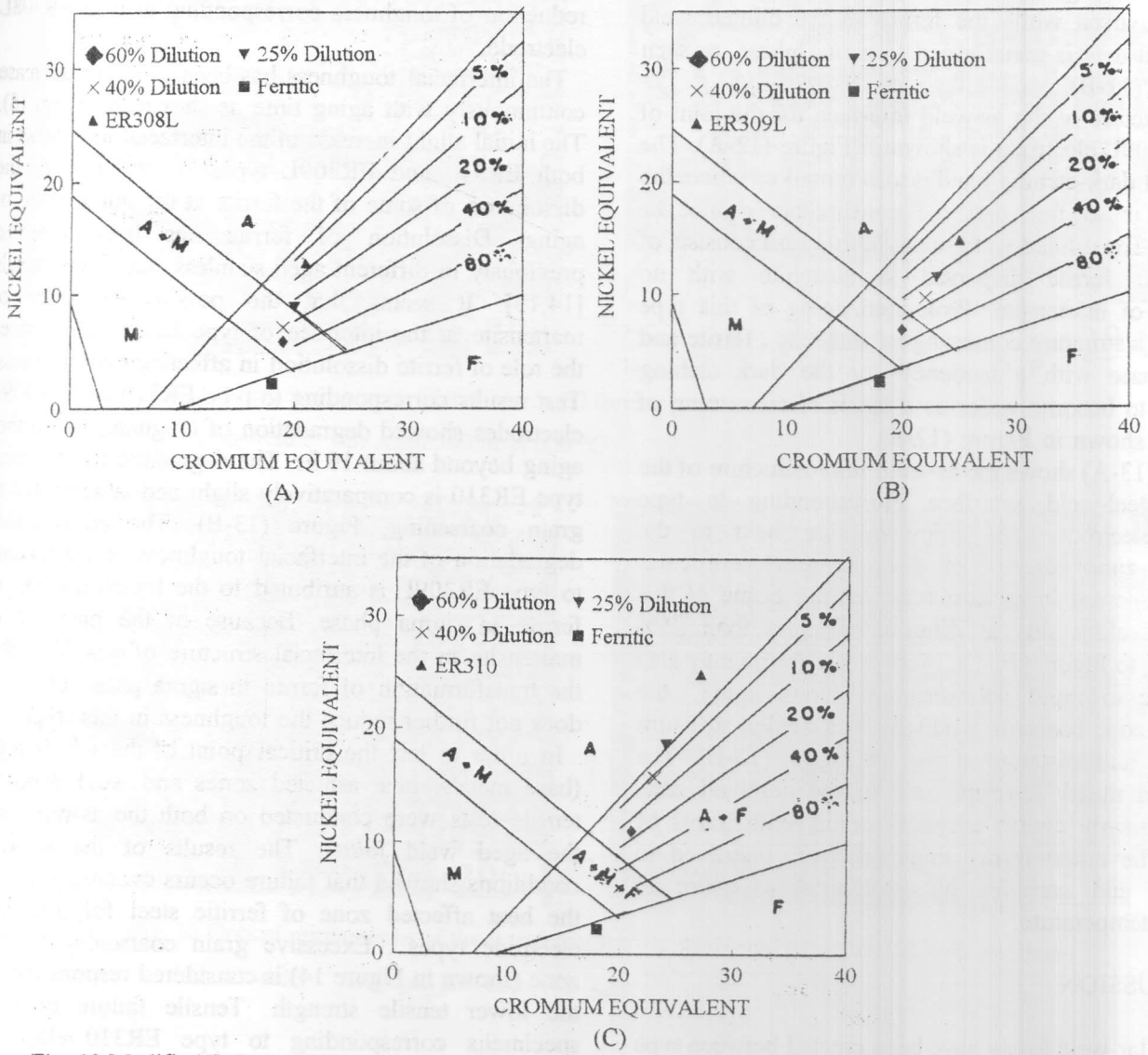

Fig. 10 Modified DeLong diagram showing the effect of dilution on the composition of ferrite-weld interface

The as-weld interfacial structure of the joint corresponding to type ER308L electrode is shown in Figure (11-A). The micrograph shows a clearly distinct dark etching band known as the unmixed zone[3, 12]. Because of the rapid solidification rate at the interface, the structure of this zone is extremely fine and the constituents could not be resolved at this magnification. Next to this zone, the microstructure of the diluted weld metal consists of continuos vermicular ferrite(gray etching) plus little martensite(dark etching) both dispersed in austenitic matrix(white etching). The vermicular ferrite morphology is typical of austenitic stainless steel weld metals of high ferrite number [12, 13] . Upon aging, the structure of the unmixed zone is seen to coarsen while the ferrite in the diluted weld metal next to it is transformed to sigma phase, as seen in Figure (11-B).

The structure of the as-weld interface for the joint of type ER309L electrode is shown in Figure (12-A). The interfacial dark-etching band is also remarked where the structure is so fine that the constituents cannot be resolved. The diluted weld metal in this case consists of vermicular ferrite dispersed in austenite with no evidence of martensite. Prolonged aging of this type results in a structure consisting of austenite , ferrite and sigma phase with a tendency for the dark etching interface to become wider as a result of coarsening of ferrite as shown in Figure (12-B).

Figure (13-A) shows the as-weld microstructure of the ferritic steel-weld interface corresponding to type ER310 electrode. The microstructure next to the unmixed zone consists of discontinuous vermicular ferrite dispersed in an austenitic matrix. Some of this ferrite develops due to dilution of more than 25% according to Figure (10-C). Meta-stable ferrite may also form due to rapid solidification. Upon aging,, the unmixed zone coarsens gradually to a duplex structure of ferrite and austenite shown in Figure (13-B). The aged-weld metal structure next to the unmixed zone showed mainly coarse austenite grains with traces of ferrite. The initial ferrite must has been dissolved to austenite and carbides by prolonged exposure at elevated temperature.

4. DISCUSSION

Dissimilar weld joints have been created between type 304 austenitic steel and type 430 ferritic steel by GTA using three different electrodes being ER308L, ER309L and ER310. Charpy test results on the as-weld specimens revealed that the critical section of the ***weld deposit*** is the interface between the ferrite and the weld metal. The interfacial toughness of the joint made using type ER310 electrode is higher than that of the other two types as concluded from Figure (6). This is attributed to the different interfacial microstructures developed by dilution as explained above (Figures 10&13). The relatively higher percentage of interfacial ferrite developed using types ER308L and ER309L is considered responsible for the lower as-weld toughness. The presence of martensite in the structure of the ***as-weld*** interface further contributes towards the reduction of toughness corresponding to type ER308L electrode.

The interfacial toughness has been found to decrease continuously with aging time as shown in Figure (8). The initial slight increase of the interfacial toughness in both ER310 and ER309L types is attributed to the dissolution of some of the ferrite at the initial stage of aging. Dissolution of ferrite has been reported previously in different aged stainless steel weld metals [14,15]. It seems that the possible presence of martensite at the interface of type ER 308L balances the role of ferrite dissolution in affecting the toughness. Test results corresponding to type ER310 and ER309L electrodes showed degradation of toughness by further aging beyond about 10 hr. The degradation concerning type ER310 is comparatively slight and is attributed to grain coarsening, Figure (13-B). The considerable degradation of the interfacial toughness corresponding to type ER309L is attributed to the transformation of ferrite to sigma phase. Because of the presence of martensite in the interfacial structure of type ER308L, the transformation of ferrite to sigma phase by aging does not further reduce the toughness in this type.

In order to test the critical point of the ***whole joint*** (base metals, heat affected zones and weld deposit), tensile tests were conducted on both the as-weld and the aged weld ***joints***. The results of the ***as-weld*** conditions showed that failure occurs eventually inside the heat affected zone of ferritic steel for the three electrode types . Excessive grain coarsening in this zone (shown in Figure 14) is considered responsible for the lower tensile strength. Tensile failure of aged specimens corresponding to type ER310 electrode occurs eventually inside the heat affected zone of

ferrite. The lower ferrite content in the diluted zone in this type together with the lower chromium content of this ferrite inhibits transformation of ferrite to the brittle constituents such as sigma phase[15]. Referring to Figure (9), the trend of the curve corresponding to type ER308L showed that the interfacial tensile strength decreases gradually with aging. It starts to decrease below the strength of ferrite HAZ at an aging time of about 20 hr. At an aging time of 8 hr or less the weld joints failed in tension inside the HAZ of ferritic steel. The trend of the curve corresponding to type ER309L (Figure 9) implies that the strength of the interface has been suddenly reduced between aging times of 8 hr and 20 hr. The decrease of strength of HAZ beyond 20 hr aging time is also attributed to the transformation to sigma phase. This transformation is accelerated by the higher ferrite content and higher chromium of ferrite corresponding to this type of electrode.

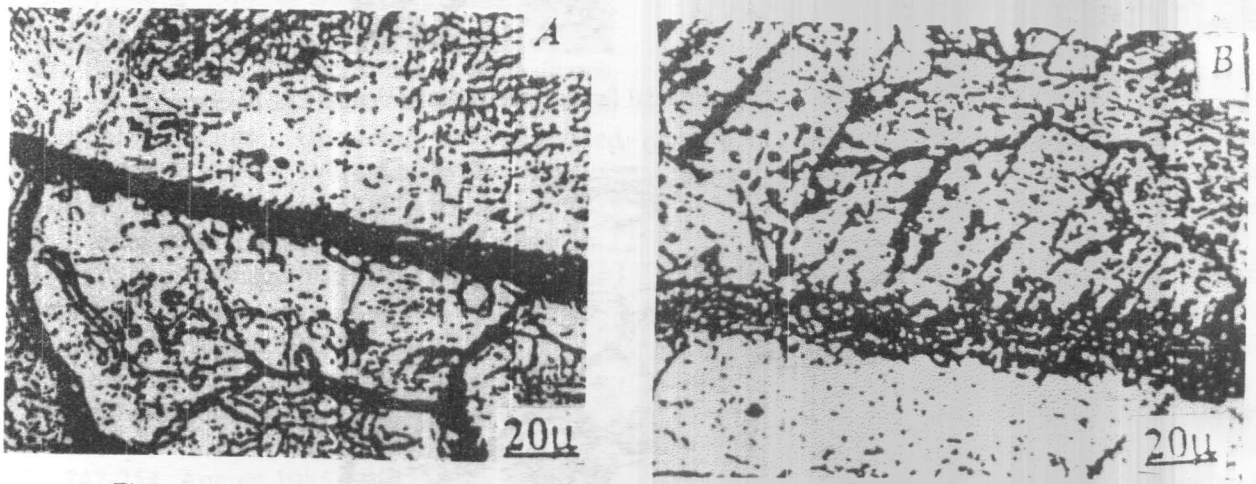

Fig. 11 Optical micrographs of the interfacial ferritic steel-weld structure(ER308L electrode)

A) As-weld B) Aged 300 hr at 600 °C

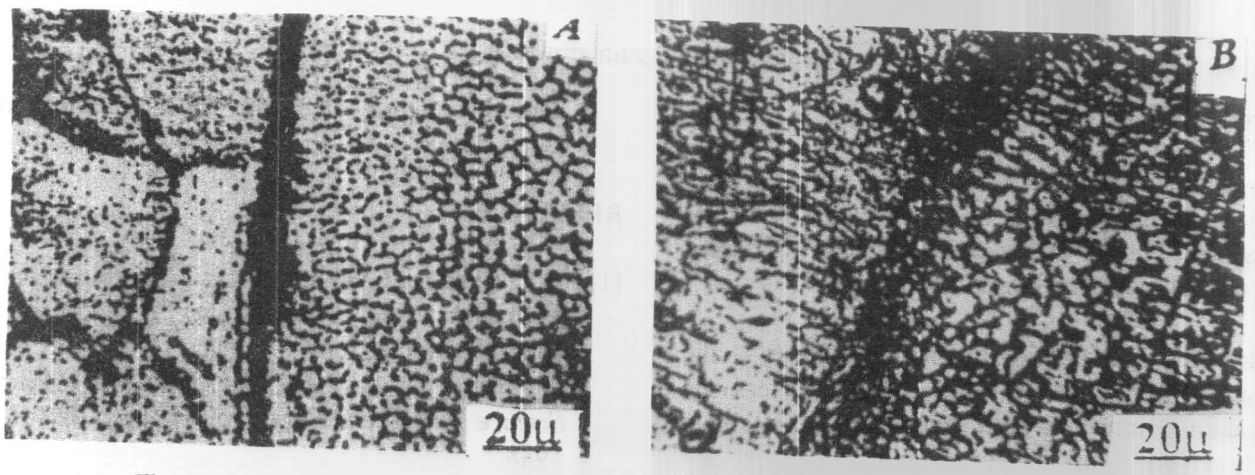

Fig. 12 Optical micrographs of the interfacial ferritic steel-weld structure(ER309L electrode)

A) As-weld B) Aged 300 hr at 600 °C

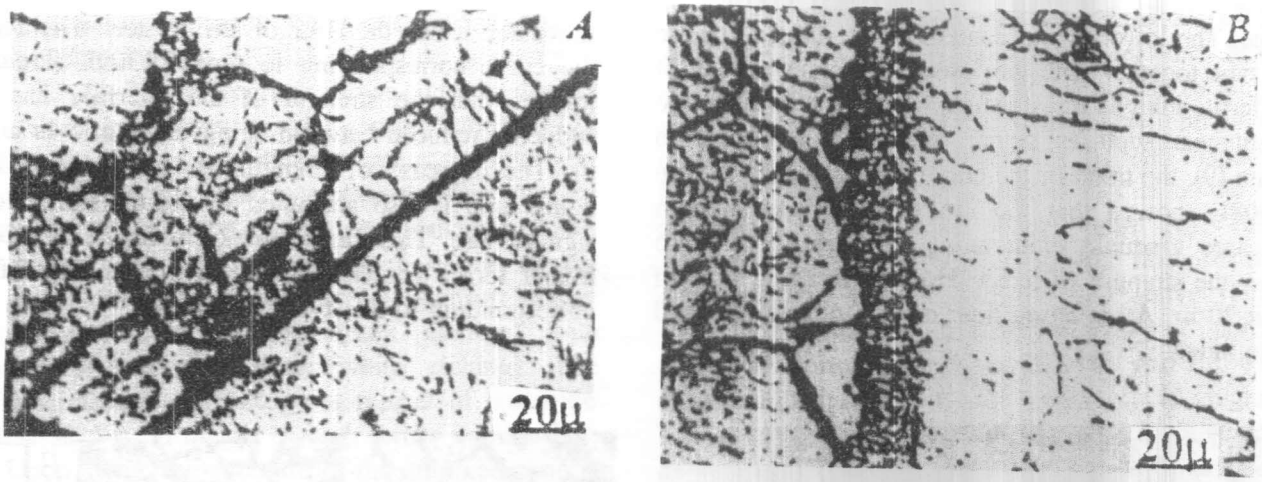

Fig. 13 Optical micrographs of the interfacial ferritic steel-weld structure(ER310 electrode)
A) As-weld B) Aged 300 hr at 600 °C

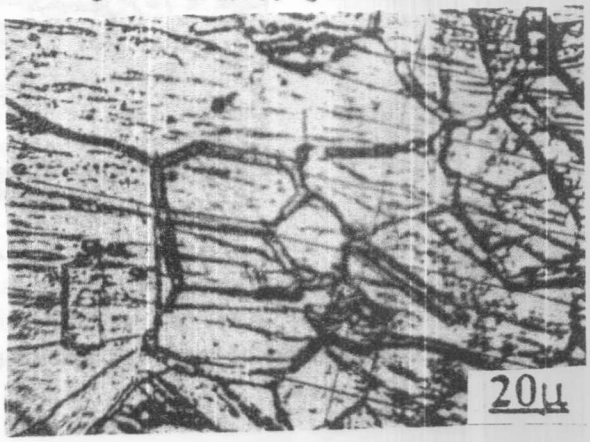

Fig. 14 Micrographs showing grain growth at HAZ of ferritic steel

5. CONCLUSION

Investigation of the dissimilar fusion joints between type 304 austenitic stainless steel and type 430 ferritic stainless steel both in the as-weld and aged conditions lead to the following conclusions:

[1] The critical section of the as-weld ***joints*** is the heat affected zone of ferritic steel, whereas the weakest point of as-weld ***deposits*** is the interface between weld metal and ferritic steel base metal.

[2] The aged ferritic-weld interface corresponding to types ER309L and ER308L electrodes has been the location of tensile failure when aging time exceeded 8 hr.

[3] The toughness of the aged ferritic-weld interface corresponding to type ER310 showed the least degradation, with a tendency for stabilization, with aging time.

REFRENCES

[1] A.K. Bhaduri, I. Gowerisankar, V. Seetharaman, S. Venkadesan and P. Rodriguez, "Development of Transition Metal Joint for Steam Generator Circuit of Prototype Fast Breeder Reactor", *Material Science and Technology*, vol. 4, pp. 1020-1029, 1988.

[2] R.E. Avery, "Pay Attention to Dissimilar Metal Welds", *Chemical Engineering Progress*, pp. 70-75, May 1991.

[3] A.K. Bhaduri, V. Seetharaman and S. Venkadesan, "Effect of Aging on the Interfacial Microstructure and Mechanical Properties of a

Alloy 800 / 2.25 Cr -1Mo Steel Joint", *Z. Metallkde*, Bd 80 H.9, pp. 630-634, October 1989.

[4] L.. Groud, *Principle of Welding Technology*, John Wiley, First edition 1980.

[5] R.D. Nicholson, "Interfacial Structure in Nickel-Based Transition Joints after Long Term Service", *Report Presented at the Welding Institute Seminar* , Leicester, England, June 1981.

[6] R.D. Nicholson and A.T. Price, "Service Experience of Nickel Based Transition Joints", *Report Presented at the Welding Institute Seminar*, Leicester, England, June 1981.

[7] B.L. Bagnall, R.G. Rowberry and J. A. Williams, "Service Experience with Heavy Section Dissimilar Joints Operating at Elevated Temperature", *Report Presented at the Welding Institute Seminar*, Leicester, England, June 1981.

[8] R. Viswanathan, "Dissimilar Metal Weld and Boiler Creep Damage Evaluation for Plant Life Extension", *Transactions of the ASME*, vol. 107, pp. 218-225, August 1985.

[9] D.I. Roberts, R. H. Ryder and R. Viswanathan, "Performance of Dissimilar Welds in Service", *Journal of Pressure Vessels Technology*, vol. 107, pp. 247-254, August 1985.

[10] Chilton, A.T. Price and B. Wilshire, "Creep Deformation and Local Strain distributions in Dissimilar Metal Welds between AISI Type 316 and 2.25Cr-1Mo Steels Made with 17Cr-8Ni-2Mo Weld Metal", *Metals Technology*, vol. 11, pp. 383-391, September 1984.

[11] Zheng and H. Huai-Yue, "Thermal Fatigue Behavior of Dissimilar Stainless Steel", *International Journal of Joining of Materials*, vol. 6 N 2-3, pp. 81-84, Sep. 1995

[12] J.C. Lippold, and W.F. Savage, "Solidification of Austenitic Stainless Steel Weldments: Part 2-The Effect of Alloy Composition on Alloy Morphology". *Welding J.*, vol. 59, pp. 48-s-58-s, Feb. 1980

[13] S.A. David, "Ferrite Morphology and Variations in Ferrite Content in Austenitic Stainless Steel Welds", *Welding J.*, vol. 60, pp. 63-s-71-s, Apr. 1981.

[14] J.M. Vitek and S.A. David, "The solidification and Aging Behavior of Type 308 and 308CRE Stainless Steel Welds", *Welding J.*, vol. 24, pp. 246-s-253-s, 1984.

[15] G.A. Nassef, "Aging Kinetics of Type 308L Stainless Steel Weld Metal", *In the "6th International Conference of Production Engineering, Design and Control*, vol. 1, pp. 279-288, Alexandria 15-17 Feb. 1997.